RUNHETC-06-02

Universal scaling behavior of the single electron box in the strong tunneling limit

Sergei L. Lukyanov
NHETC, Department of Physics and Astronomy, Rutgers University, Piscataway, NJ 08855-0849, USA
and
L.D. Landau Institute for Theoretical Physics Chernogolovka, 142432, Russia

Philipp Werner
Department of Physics, Columbia University, 538 West, 120th Street, New York, NY 10027

(Dated: June 16, 2006)

We perform a numerical analysis of recently proposed scaling functions for the single electron box. Specifically, we study the "magnetic" susceptibility as a function of tunneling conductance and gate charge, and the effective charging energy at zero gate charge as a function of tunneling conductance in the strong tunneling limit. Our Monte Carlo results confirm the accuracy of the theoretical predictions.

I. INTRODUCTION

A single electron box is a low-capacitance metallic island, connected to an outside lead by a tunnel junction. It has first been experimentally realized by Lafarge and co-workers [1]. Such a device exhibits Coulomb-blockade phenomena due to the large charging energy, which influences single electron tunneling. By applying a gate voltage V_G it is possible to induce a continuous polarization charge $n_G = C_G V_G/e$ on the island (see Fig. 1). For a very small dimensionless tunneling conductance $\alpha = h/(2\pi^2 e^2 R_t) \ll 1$ (R_t is the resistance of the contact) the energy spectrum is given by the set of parabolas $E_n(n_G) = E_C(n - n_G)^2$, where the integer n denotes the number of excess electrons. $E_C = e^2/2(C_t + C_G)$ is the single electron charging energy, which sets the energy scale. As the tunneling conductance is increased, quantum fluctuations lead to a renormalized *effective* charging energy E_C^*. The properties of the electron box for $\alpha \lesssim 0.8$ are well described by perturbation theory in α, and these results have been verified numerically [2].

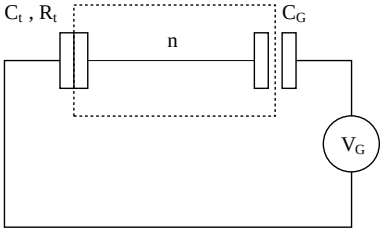

FIG. 1: Circuit diagram of the single electron box. The box with excess charge n is indicated by the dashed rectangle. It is connected to a voltage source through a capacitor C_G and a tunnel junction with resistance R_t and capacitance C_t.

Over the last decade, the analytical expressions describing a single electron box in the limit of large tunneling conductance have been the subject of controversial debate [3,4,5,6,7]. Numerical investigations which were performed to test the numerous incompatible predictions have proven difficult or inconclusive, and in some cases even added to the confusion [5,8,9,10,11]. It is the purpose of this paper to remedy this unsatisfactory state of affairs and present a comprehensive study of recently obtained scaling formulas, using state-of-the-art numerical techniques.

II. THEORY

We address the limit of large tunneling conductance in the framework of the Ambegaokar-Eckern-Schön model [12,13]. The partition function for the model can be written as a path integral over an angular variable ϕ (conjugate to the number of excess charges on the island)

$$Z = \int \mathcal{D}\phi \; \mathrm{e}^{-\mathcal{A}[\phi]} \,, \tag{1}$$

where the Matsubara effective action reads ($\hbar = 1$ and β denotes the inverse temperature)

$$\begin{aligned} \mathcal{A}[\phi] \;&=\; \frac{1}{4E_C}\int_0^\beta \mathrm{d}\tau\,(\partial_\tau\phi)^2 + \mathrm{i}\,n_G\int_0^\beta \mathrm{d}\tau\,\partial_\tau\phi \\ &+\; \frac{\alpha\pi^2}{\beta^2}\int_0^\beta\int_0^\beta \mathrm{d}\tau\mathrm{d}\tau'\,\frac{\sin^2(\frac{\phi(\tau)-\phi(\tau')}{2})}{\sin^2(\frac{\pi}{\beta}(\tau-\tau'))}\,. \end{aligned} \tag{2}$$

The first two terms account for the charging effect, whereas the third, "dissipative" term describes the electron tunneling. Introducing a two component unit vector $\boldsymbol{S} = (\cos\phi\,,\,\sin\phi)$ at any point of the Matsubara circle, $\mathcal{A}[\phi]$ can be viewed as the classical energy of the XY model with long range interaction [14]. The first term in Eq. (2) is then identical to the spin wave approximation to an extra short range interaction. Finally, the term $\propto n_G$ acts like a purely imaginary external torque on the XY spins.

We are primarily interested in the "magnetic" susceptibility and effective charging energy of the model (2). By magnetic susceptibility we mean the quantity

$$\chi_m = \frac{2}{\beta^2} \int_0^\beta \int_0^\beta \mathrm{d}\tau \mathrm{d}\tau' \, \left\langle S_x(\tau) S_x(\tau') \right\rangle \, , \qquad (3)$$

characterizing the linear response of the spin chain to an external "magnetic" field coupled to $S_x \equiv \cos\phi$. The effective charging energy, in turn, is defined as

$$E_C^* = -\frac{1}{2\beta} \, \frac{\partial^2}{\partial n_G^2} \, \log(Z) \, . \qquad (4)$$

In the terminology of QFT a quantity like (4) is usually referred to as a *topological* susceptibility because of the topological nature of the second term in Eq. (2), and the parameter

$$\theta = 2\pi n_G \qquad (5)$$

is called the topological angle.

When both βE_C, $\alpha \to \infty$ the model (2) develops a universal scaling behavior characterized by the energy scale E^* (Kondo temperature). In this regime $g_0 = (2\pi^2\alpha)^{-1}$ plays the role of the bare perturbative coupling and the first term in Eq. (2) just provides an explicit ultraviolet cut-off of the dissipative action, with the cut-off energy

$$\Lambda = 2\pi^2 \, E_C \, \alpha \, . \qquad (6)$$

The Kondo temperature admits a perturbative expansion of the form [5,14]

$$E^* \simeq 2\pi^2 E_C \, \alpha^2 \, \mathrm{e}^{-\alpha\pi^2} \, \Big(1 + \sum_{k=1}^{\infty} b_k \, \alpha^{-k} \Big) \, , \qquad (7)$$

where the symbol $\simeq$ stands for asymptotic equality. While the overall factor $2\pi^2$ in Eq. (7) is a matter of convention, all the expansion coefficients b_k are determined unambiguously within the standard perturbation theory. In particular [7]

$$b_1 = -\frac{3}{8} \, . \qquad (8)$$

In the scaling limit, i.e., in the limit when $\Lambda \to \infty$, $\alpha \to \infty$ with the energy scale E^* kept fixed, the magnetic susceptibility (3) is expected to possess the normal scaling behavior of the form [7]

$$\chi_m = \frac{1}{2\pi^2 \alpha} \, \Big[\, F_m(\kappa, \theta) + O\big((\beta\Lambda)^{-1} \big) \Big] \, , \qquad (9)$$

where the parameter κ is the inverse temperature measured in units of the Kondo temperature,

$$\kappa = \beta E^* \, , \qquad (10)$$

and the topological angle θ is given by Eq. (5).

The scaling behavior of the effective charging energy (4) is a more delicate issue. Let us note at this point that field theories possessing topologically nontrivial classical Euclidean solutions (instantons) usually suffer from specific "instanton divergences". The phenomenon was originally observed in 4D QCD [15]. Later it was extensively studied in the context of the 2D $O(3)$ nonlinear σ-model [16,17,18,19]. For $E_C = \infty$, the model (2) admits instanton solutions [20] which result in the "small instanton problem" (see the appendix below). For large but finite E_C the Coulomb term not only makes the theory perturbatively well-defined, but also regularizes the "small instanton divergence". As $E_C \to \infty$, the divergence restores and entails the anomalous scaling behavior for the effective charging energy [7]:

$$E_C^* = 2\pi^2 E^* \, \big[\, L \, \cos(\theta) + F_t(\kappa, \theta) + o(1) \, \big] . \qquad (11)$$

Here L is a temperature-independent constant, diverging when $\alpha \to \infty$ and $o(1)$ is a correction which vanishes in this limit. The scaling function F_t is defined modulo a transformation $F_t \to F_t + c \, \cos\theta$, since any finite constant c can be absorbed by the divergent term. This ambiguity can be resolved by imposing a proper normalization condition, say,

$$\lim_{\kappa \to \infty} F_t(\kappa, 0) = 0 \, . \qquad (12)$$

As soon as the normalization of F_t is chosen, the divergent term in Eq. (11) is also defined unambiguously. According to the result of Ref. [7]

$$L(\alpha) = 2\pi^2 \alpha - 5 \, \log\alpha - C \, . \qquad (13)$$

The constant C has been found recently in Ref. [22]:

$$C = 5\,\gamma_E + 6 \, \log 2 + 10 \, \log\pi = 18.492\ldots \, , \qquad (14)$$

where $\gamma_E = 0.5772\ldots$ is Euler's constant.

As was argued in Refs. [7,21,22], the scaling behavior of thermodynamic functions of the model (2) can be described in terms of solutions of the differential equation

$$\Big[\, -\partial_y^2 + \kappa^2 \, \exp\big(\mathrm{e}^y \big) - \kappa^2 \sin^2(\theta) \Big] \, \Psi(y) = 0 \, . \qquad (15)$$

Namely, let Ψ_+ and Ψ_- be solutions of Eq. (15) which are fixed by the asymptotic conditions

$$\Psi_-(y) \to \mathrm{e}^{y\kappa\cos\theta} \, , \quad y \to -\infty \qquad (16)$$

and

$$\Psi_+(y) \to \sqrt{\frac{\pi}{\kappa}} \, \exp\Big[\, -\tfrac{1}{4}\mathrm{e}^y - \kappa \, \mathrm{Ei}\big(\tfrac{\mathrm{e}^y}{2}\big) \Big] , \quad y \to +\infty \qquad (17)$$

with $\mathrm{Ei}(z) = \int_{-z}^{\infty} \frac{\mathrm{d}x}{x} \, \mathrm{e}^{-x}$. Then the scaling function F_t defined in Eq. (11), satisfying the normalization condition (12), reads as follows [22]:

$$F_t(\kappa, \theta) = -\kappa^{-1} \, \partial_\theta^2 \log \bar{Z}(\kappa, \theta) \, , \qquad (18)$$

where

$$\bar{Z}(\kappa,\theta) \;=\; \frac{(2\mathrm{e}^{\gamma_E}\kappa^2)^{\kappa\cos\theta}}{\Gamma(1+2\kappa\cos\theta)}\; W[\Psi_+,\Psi_-]\;, \qquad (19)$$

and $W[\Psi_+,\Psi_-] = \Psi_+\partial_y\Psi_- - \Psi_-\partial_y\Psi_+$ is the Wronskian of the solutions $\Psi_+(y)$ and $\Psi_-(y)$. It should be emphasized that Ψ_- can be defined by means of the asymptotic condition (16) for $0 \le \theta < \frac{\pi}{2}$ only. For $\frac{\pi}{2} < \theta \le \pi$, the solution Ψ_- grows at large negative y and the asymptotic formula (16) does not define Ψ_- unambiguously. It is possible to show that the function $\Psi_-/\Gamma(1+2\kappa\cos\theta)$ is an entire function of the complex variable $\zeta = \cos\theta$ for real y. So the solution $\Psi_-(y)$ can be introduced within $\frac{\pi}{2} \le \theta \le \pi$ through analytic continuation with respect to the variable θ from the domain $0 \le \theta < \frac{\pi}{2}$.

The scaling functions $F_m(\kappa,\theta)$ defined in Eq. (9) were proposed for the cases $\theta = 0$ and $\theta = \pi$ in Refs. [7] and [21], respectively. These results can be summarized as follows. Let us introduce the function

$$M(\kappa,\theta) = A_+(y) + A_-(y) + \frac{\partial_y A_+(y) - \partial_y A_-(y)}{s_+(y) - s_-(y)}\,, \qquad (20)$$

where $s_\pm(y) = \partial_y \log\Psi_\pm(y)$ and

$$\begin{aligned} A_+(y) \;&=\; \int_y^\infty \frac{\mathrm{d}u}{\Psi_+^2(u)} \int_u^\infty \mathrm{d}v\, \mathrm{e}^v\, \Psi_+^2(v)\;, \\ A_-(y) \;&=\; \int_{-\infty}^y \frac{\mathrm{d}u}{\Psi_-^2(u)} \int_{-\infty}^u \mathrm{d}v\, \mathrm{e}^v\, \Psi_-^2(v)\;. \end{aligned} \qquad (21)$$

Notice that the RHS in Eq. (20) does not actually depend on the choice of y. Then

$$F_m(\kappa,\theta) = M(\kappa,\theta) \quad \text{with} \quad \theta = 0 \;\text{ and }\; \pi\;. \qquad (22)$$

It is essential to point out that no arguments have been given that relation (22) holds true for any values of θ different from $\theta = 0$ and $\theta = \pi$.

Let us now turn to the expression for the effective charging energy at zero temperature and gate charge. Eqs. (11-13) imply that

$$\left.\frac{E_C^*}{E_C}\right|_{n_G=\beta^{-1}=0} \;\simeq\; f(\alpha)\;\mathrm{e}^{-\alpha\pi^2} \quad \text{as} \quad \alpha\to\infty\;, \qquad (23)$$

where

$$f(\alpha) = 4\pi^4\alpha^2\,\big[\,1 - \tfrac{3}{8\alpha} + O(\alpha^{-2})\,\big]\,\big[\,L(\alpha) + o(1)\,\big]\,, \qquad (24)$$

and $L(\alpha)$ is given by Eq. (13).

There is a controversy in the literature about the asymptotic behavior of E_C^* at $n_G = \beta^{-1} = 0$ in the large-α limit. All the predictions agree on the exponential suppression of the effective charging energy, but there are numerous conflicting results for the leading term of the pre-exponential factor $f(\alpha)$, with powers ranging from α^1 to $\alpha^{6.5}$ [3,4,5,6,9]. Several attempts to resolve the issue by numerical simulations [5,8,10] have failed because of the difficulty to reach the large-α regime where the exponential factor in Eq. (23) dominates. Using efficient algorithms, it is possible to compute the effective charging energy at essentially zero temperature for $\alpha \lesssim 2$ [11]. In this range of α's, there was no obvious agreement with any of the theoretically predicted asymptotic formulas. While the pre-exponential factors of Refs. [3,5,9] could be ruled out on the basis of the numerical results presented in Ref. [11], no definite conclusion could be reached concerning the predictions of Refs. [4,7]. It should be noted that the value of the constant C defined in Eq. (14) was not available at that time.

The goal of the present work is to verify the analytical results quoted above, including expression (24), by means of Monte Carlo simulations.

III. NUMERICAL METHOD

In order to simulate the electron box, we map the system (2) for $n_G = 0$ to a finite chain of classical XY spins, by discretizing imaginary time into N equal slices $\Delta\tau = \beta/N$,

$$\begin{aligned} \mathcal{A}_{\mathrm{XY}}[\phi] \;&=\; \frac{1}{2E_C\Delta\tau}\;\sum_{k=1}^{N}\big(1-\cos(\phi_{k+1}-\phi_k)\,\big) \\ &+\; \frac{\alpha\pi^2}{N^2}\;\sum_{k<k'}\frac{1-\cos(\phi_k-\phi_{k'})}{\sin^2(\frac{\pi}{N}(k-k'))}\;. \end{aligned} \qquad (25)$$

The quasiperiodic boundary condition $\phi_{N+1} = \phi_1 + 2\pi w$ is employed. In fact, the simulation treats the phases as compact variables and the winding number w is computed by summing up the phase differences (between neighboring spins) along the chain. These phase differences are defined modulo 2π and we use the smaller angle – a procedure which should yield accurate results for sufficiently small time steps (see also comments in section IV B).

The effective charging energy at gate charge zero can be computed from the winding numbers w of the paths ϕ and the corresponding weights P_w – the probabilities for a given w [5]:

$$\left.\frac{E_C^*}{E_C}\right|_{n_G=0} = \frac{2\pi^2}{\beta E_C}\;\frac{\sum_w w^2\,P_w}{\sum_w P_w}\;. \qquad (26)$$

Results for non-zero gate charge can be obtained from the expectation values $\langle\cdots\rangle_w$ in the different winding sectors w:

$$\langle\,\mathcal{O}\,\rangle = \frac{\sum_w \mathrm{e}^{2\pi\mathrm{i}wn_G}\;P_w\,\langle\,\mathcal{O}\,\rangle_w}{\sum_w \mathrm{e}^{2\pi\mathrm{i}wn_G}\;P_w}. \qquad (27)$$

Because of cancellation effects due to the phase factors in Eq. (27), the error bars can grow rapidly as a function of n_G, especially at small α, where the P_w-distribution is very broad. This manifestation of a sign problem restricts the parameter range for which accurate results can be obtained.

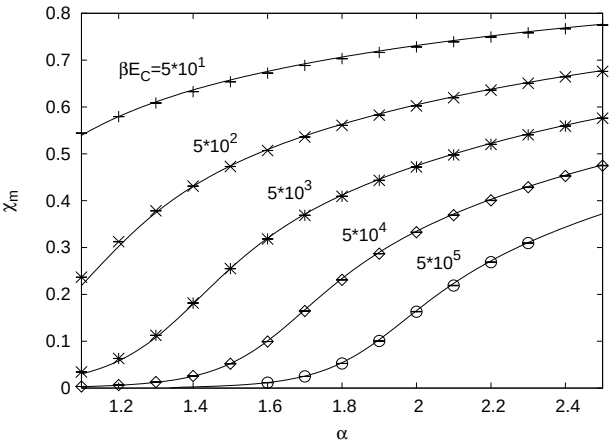

FIG. 2: Comparison of $\frac{1}{2\pi^2\alpha}\ M(\kappa,0)$ defined in Eq. (20) (lines) and Monte Carlo results (symbols) for χ_m (Eq. (3), $n_G=0$). The numerical data, which include error bars, were obtained for $\Delta\tau E_C = 0.05$.

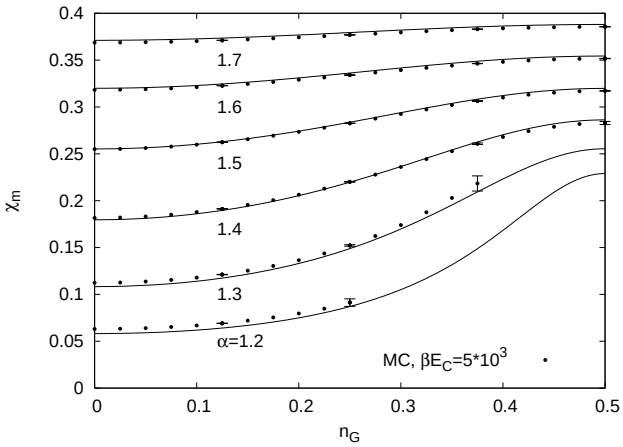

FIG. 3: $\frac{1}{2\pi^2\alpha}\ M(\kappa,2\pi n_G)$ defined in Eqs. (20) (lines) and Monte Carlo results (symbols) for χ_m (3) and several values of α. The numerical data were obtained for $\beta E_C = 5\cdot 10^3$ and $\Delta\tau E_C = 0.05$; error bars at $n_G = 0.125$, 0.25, 0.375 and 0.5 indicate the accuracy.

We use Wolff cluster updates with efficient treatment of long range interactions [23,24] in our Monte Carlo simulations. This algorithm builds clusters in a time $O(N\log N)$ and allows us to simulate chains of up to 10^7 spins. For a discretization step $\Delta\tau E_C = 0.05$ it is therefore possible to reach temperatures down to $\beta E_C = 5\cdot 10^5$.

IV. RESULTS

A. Magnetic susceptibility

In Fig. 2 we compare the Monte Carlo results for the magnetic susceptibility for $n_G = 0$ against the scaling form (9), (22). The plot for $n_G = \frac{1}{2}$ ($\theta = \pi$) looks pretty much the same as Fig. 2. Note that we applied relations (7), (8), (10) to find the value of the scaling parameter κ corresponding to a given α and βE_C. The agreement between the analytical prediction and Monte Carlo results is within $\sim 0.5\%$ for $\beta E_C = 5\times 10^n$, $n = 1, 2, 3$ and within $\sim 1-2\%$ for $\beta E_C = 5\times 10^n$, $n = 4, 5$. Among other things, this indicates that the asymptotic series (7) truncated at $k = 1$ approximates the Kondo temperature E^* with an estimated error $\lesssim 1\%$ for any $\alpha > 1$. This level of accuracy seems reasonable given that the $k = 1$ term leads to a correction of approximately 10% for these α.

As has been mentioned above there is no strong theoretical argument that relation (22) is satisfied for $\theta \in [0,\pi]$. However, as shown in the appendix, the saddle point approximation for χ_m is consistent with the hypothesis that the relation holds true for any $\theta \in [0,\pi]$. Further evidence that Eq. (22) is satisfied for all θ comes from the study of the zero-temperature limit of the scaling function $F_m(\kappa,\theta)$. Namely, as follows from (3), (9), there exists a limit

$$\lim_{\kappa\to\infty}\big(\kappa\, F_m(\kappa,\theta)\big) = f_m(\theta)\ . \tag{28}$$

Here $f_m(\theta)$ is some function of the single variable θ which possesses a singular behavior as $\theta\to\pi$. Using results of Refs. [21,22] one can show that

$$f_m(\theta) \to \frac{\pi}{\pi-\theta} \quad \text{as} \quad \pi-\theta\to+0\ . \tag{29}$$

At the same time, with the WKB approximation it is not difficult to prove the relation

$$\lim_{\kappa\to\infty}\big(\kappa\, M(\kappa,\theta)\big) = \frac{\theta}{\sin(\theta)}\ . \tag{30}$$

Apparently Eqs. (28), (29) and (30) are consistent with the conjecture $F_m(\kappa,\theta) = M(\kappa,\theta)$.

For the above reasons, we found it natural to test Eq. (22) numerically. The result is depicted in Fig. 3. The missing data points for $\alpha = 1.2$ and 1.3 fell victim to the sign problem mentioned in the previous section. This sign problem prevents us from investigating the singularity at $\theta = \pi$, which appears in the limit $T\to 0$.

B. Effective charging energy for zero gate charge

First of all it is instructive to determine a range of temperatures appropriate for numerical tests of the scaling relation (11). The leading temperature-dependent correction to Eq. (11) readily follows from the saddle point calculations presented in the appendix. Those calculations suggest (see formula (A16)) to replace the temperature-independent constant $L = L(\alpha)$ (13) by

$$L(\alpha,\beta E_C) = L(\alpha) + L_1\big(\tfrac{2\pi^2}{\beta E_C}\big)\ , \tag{31}$$

with

$$L_1(x) = 2\,\mathrm{e}^{\frac{x}{2}}\ \mathrm{Ei}(-x) + 2\,\log\left(x\mathrm{e}^{\gamma_E}\right)\ . \qquad (32)$$

For $\beta E_C = 5{\cdot}10^1$, the term L_1 turns out to be fairly large (≈ 1.0). For this reason, it makes no sense to use Monte Carlo data with $\beta E_C = 5\cdot 10^1$ to test the relation (11). In the case $\beta E_C = 5\cdot 10^2$, $L_1 \approx 0.2$, so the correction is small but still visible and it is useful to take it into account. For $\beta E_C = 5\cdot 10^n$ with $n \geq 3$, the term L_1 in Eq. (31) is smaller than the error bars of our Monte Carlo data (< 0.03), and thus negligible.

In Ref. [11] it was noted that the disagreement between previous Monte Carlo results [5,8,10] for E_C^* at $\alpha \gtrsim 1$ were due to lattice effects. Therefore it is very important to take proper care of the systematic errors introduced by the imaginary time discretization in the calculation of E_C^*.

As a matter of fact, the strong effect of the discretization on the topological susceptibility is well known in the context of the 2D $O(3)$ nonlinear σ-model [17,18,19]. The primary reason of this effect is that strictly speaking the concept of winding number in a lattice formulation breaks down. In a discretized theory every field configuration can be continuously transformed into any other. If lattice configurations are sufficiently smooth, an unambiguous topological charge may be assigned. Conversely, for field configurations containing large fluctuations the interpolation is not unique and the winding number definition becomes ambiguous. For finite E_C the discretized Coulomb term in the lattice action (25) suppresses the lattice configurations containing large fluctuations. However, it is possible to show that if $\alpha\,\Delta\tau E_C > 1$ then starting with non-zero charged configurations one can continuously lower the lattice action $\mathcal{A}_{\mathrm{XY}}$ to zero by a local minimization in the spin variables [25]. For this reason the divergent constant L in Eq. (11) (which is not universal and depends on details of the discretization of the action (2)) is a singular function of the lattice parameter

$$\delta = \alpha\,\Delta\tau E_C\ , \qquad (33)$$

at $\delta = 1$. Namely,

$$L \propto -2\,\log(1-\delta)\ . \qquad (34)$$

In Fig. 4, $\frac{E_C^*}{2\pi^2 E^*}$ with $n_G = 0$ is plotted as a function of $\Delta\tau E_C$ for $\beta E_C = 5\cdot 10^3$ and some values of α. An analysis of the plotted Monte Carla data suggests that the effect of the lattice discretization for $\delta \ll 1$ can be accounted for by means of the following modification of Eq. (31):

$$\begin{aligned} L(\alpha, \beta E_C, \delta) \ &= \ L(\alpha) + L_1\left(\tfrac{2\pi^2}{\beta E_C}\right) \\ &\quad -2\,\log(1-\delta) + 2\,\bar{C}\,\delta\ . \end{aligned} \qquad (35)$$

Here $L(\alpha)$ and $L_1(x)$ are given by Eqs. (13) and (32), respectively, and $\bar{C}$ is a fitting parameter. The continuous lines in Fig. 4 correspond to $\bar{C} = 2.8$.

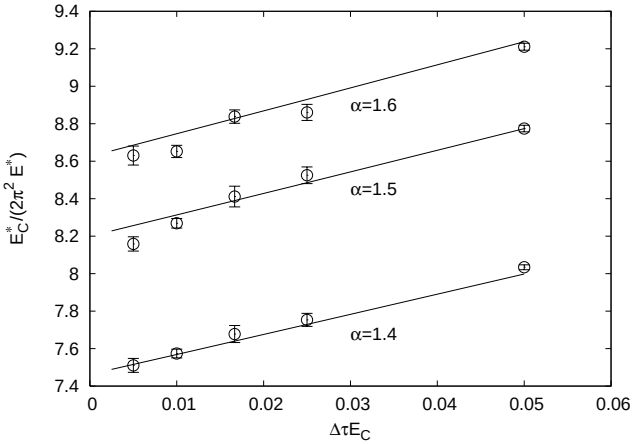

FIG. 4: Illustration of lattice effects for $\frac{E_C^*}{2\pi^2 E^*}$ ($n_G = 0$). The Monte Carlo data correspond to $\alpha = 1.4$, 1.5, 1.6 and $\beta E_C = 5\cdot 10^3$. The lines show the analytical results corresponding to the lattice fitting parameter $\bar{C} = 2.8$ in Eq. (35).

In order to minimize the impact of the non-universal temperature and lattice effects discussed above, we first study the quantity ($n_G = 0$)

$$f_{nm}(\alpha) = \left.\frac{E_C^*}{2\pi^2 E^*}\right|_{\beta E_C = 5\cdot 10^n} - \left.\frac{E_C^*}{2\pi^2 E^*}\right|_{\beta E_C = 5\cdot 10^m}\ . \qquad (36)$$

As follows from Eq. (11), the anomalous terms cancel out for such differences. Hence one should expect that the functions f_{nm} possess the normal scaling behavior of the form

$$f_{nm}(\alpha) \to F_t(\kappa_n, 0) - F_t(\kappa_m, 0)\ \ (n,\, m,\, \alpha \to \infty) \qquad (37)$$

with $\kappa_{n,m}$ the values of the scaling parameter κ (10) corresponding to a given α and $\beta E_C = 5\cdot 10^{n,m}$. Also notice that the non-universal temperature corrections to the scaling behavior (37) are expected to be sufficiently small provided $n, m \geq 3$. Since the most accurate Monte Carlo data are those for $n = 3$, we plot in Fig. 5 the result for f_{43}, obtained for a discretization step $\Delta\tau E_C = 0.05$, and the analytical prediction (Eqs. (37), (18)). The agreement is as good as it can be expected, given the errors on the Monte Carlo data, and a similar result is found for f_{32}.

In Fig. 6 the prediction (11), (18) for $n_G = 0$ and L understood as in Eq. (35), is compared to the Monte Carlo data for different values of the parameters βE_C and $\Delta\tau E_C$. The value $\bar{C} = 2.8$ has been used for all analytical curves. The agreement between the theoretical predictions and the Monte Carlo results shows that the scaling formulas (11), (13), (18) for the effective charging energy are correct. In particular, this implies that the leading power in the pre-exponential factor $f(\alpha)$ (see Eqs. (23) and (24)) is α^3.

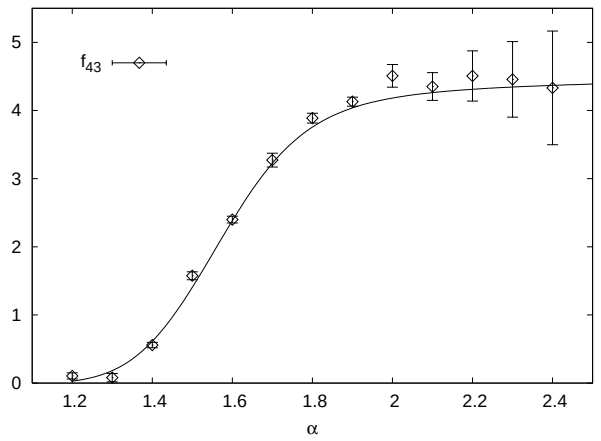

FIG. 5: Comparison of the Monte Carlo data and analytical prediction for f_{43} defined in Eq. (36). The numerical data correspond to $\Delta\tau E_C = 0.05$ and the analytical result was obtained using Eqs. (37), (18).

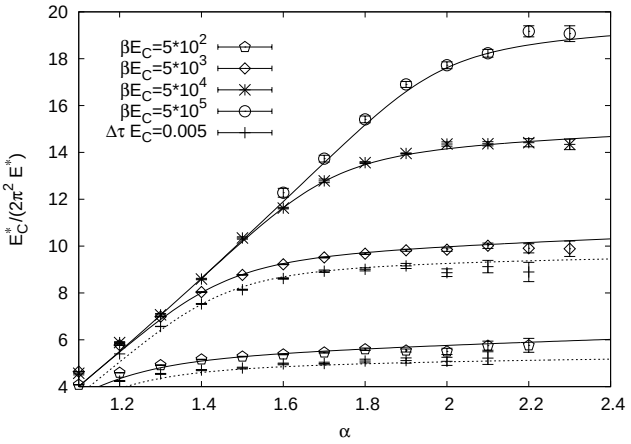

FIG. 6: Analytical prediction (lines) and Monte Carlo results (symbols) for $\frac{E_C^*}{2\pi^2 E^*}$ and several values of βE_C ($n_G = 0$). The numerical data were obtained for $\Delta\tau E_C = 0.05$ (points on solid lines) and $\Delta\tau E_C = 0.005$ (points on dotted lines). The coefficient $\bar{C} = 2.8$ (35) was used for all the analytical curves.

V. SUMMARY

We have presented scaling formulas for the single electron box in the limit of almost perfect transmission, as well as a conjecture for the gate charge dependence of the magnetic susceptibility. These analytical predictions have been tested by means of Monte Carlo simulations of the discretized action (corresponding to an XY spin chain with long range couplings) with up to 10^7 spins. Because of the lattice effects, it was necessary to introduce a constant, $\bar{C} = 2.8$, in order to compare the analytical predictions to the simulation results for the effective charging energy. But this single fitting parameter was enough to obtain a good agreement between the Monte Carlo data and the theoretical predictions over a whole range of temperatures ($5 \cdot 10^2 \le \beta E_C \le 5 \cdot 10^5$), lattice spacings ($0.005 \le \Delta\tau E_C \le 0.05$) and dissipation strengths ($1.2 \lesssim \alpha \lesssim 2.4$). These results essentially verify the scaling formulas for the effective charging energy for $n_G = 0$ presented in Ref. [22], and thus also settle the controversy surrounding the pre-exponential factor $f(\alpha)$ in Eq. (23). Unfortunately the quality of the Monte Carlo data for $E_C^*(n_G)$ with $n_G \neq 0$ was not sufficient for a meaningful test of the θ-dependence of the scaling function $F_t(\kappa, \theta)$ (11) against the theoretical prediction (18).

As for the magnetic susceptibility, our investigation suggests that some of the results from Refs. [7,21] for $n_G = 0$ and $n_G = 1/2$ can be generalized to all values of the gate charge.

Acknowledgments

The calculations have been performed on the Hreidar Beowulf cluster at ETH Zürich, using the ALPS library [26]. The authors thank M. Troyer for the generous allocation of computer time. SL is grateful to Alexander B. Zamolodchikov for previous collaborations and his interest in this work.
Research of SL is supported in part by DOE grant #DE-FG02-96 ER 40949. PW acknowledges support from NSF DMR 0431350.

APPENDIX A: SADDLE POINT APPROXIMATION

In this appendix we consider the saddle point approximation for the model (2) in the limit $E_C \to \infty$. In the absence of the first term, the local minima of the Euclidean action $\mathcal{A}[\phi]$ in the sectors with winding number $w \ge 0$ are saturated by the instanton solutions [20,27]

$$\mathrm{e}^{\mathrm{i}\phi_{\mathrm{inst}}(\tau)} = \mathrm{e}^{\mathrm{i}\phi_0} \prod_{m=1}^{w} \frac{z - z_m}{1 - z_m^* z} \quad \text{with} \quad z = \mathrm{e}^{2\mathrm{i}\pi\tau/\beta} . \tag{A1}$$

The set of complex parameters $\{z_m : |z_m| < 1\}_{m=1}^{w}$ and the real constant $0 \le \phi_0 < 2\pi$ are instanton moduli. Let us introduce an external magnetic field in the system:

$$\mathcal{A}_h[\phi] = \mathcal{A}[\phi] + h\sqrt{\alpha} \int_0^\beta \mathrm{d}\tau \, \cos\big(\phi(\tau)\big) . \tag{A2}$$

We assume that h is sufficiently small so that the additional term has no appreciable effect on the instanton solutions. Calculating the action $\mathcal{A}_h[\phi]$ for the paths (A1) yields

$$\mathcal{A}_h[\phi_{\mathrm{inst}}] = \mathrm{i}\,\theta w + \alpha\pi^2 \, w + \tfrac{1}{2}\,\beta h\sqrt{\alpha}\,(-1)^w \times \Big(\mathrm{e}^{\mathrm{i}\phi_0} \prod_{m=1}^{w} z_m + \mathrm{e}^{-\mathrm{i}\phi_0} \prod_{m=1}^{w} z_m^* \Big) , \tag{A3}$$

where θ is the topological angle (5). Within the saddle point approximation the partition function is given by

$$Z_{\rm inst}(h) = \sum_{w=0}^{\infty} \int_w {\rm d}\mathcal{M}_w \ {\rm e}^{-\mathcal{A}_h[\phi_{\rm inst}]} \ , \qquad \text{(A4)}$$

where $\int_w$ stands for the integral over the domain $0 \leq \phi_0 < 2\pi,\ |z_m| < 1$ $(m = 1, \dots w)$. The integration measure ${\rm d}\mathcal{M}_w$ should be computed as usual by integrating out the Gaussian fluctuations around the instanton solutions. It was calculated in Refs. [6,28]:

$$\begin{aligned} {\rm d}\mathcal{M}_w \ &= \ \frac{(\beta\Lambda)^w}{w!} \ (2\pi^2\alpha)^{\frac{1}{2}+w} \times \qquad \text{(A5)} \\ &\frac{{\rm d}\phi_0}{2\pi} \wedge \prod_{m=1}^{m} \frac{{\rm d}z_m \wedge {\rm d}z_m^*}{2\pi {\rm i}} \ \det \parallel G(z_i, z_j) \parallel \ . \end{aligned}$$

Here

$$G(z_i, z_j) = \frac{1}{1 - z_i z_j^*} \ , \qquad \text{(A6)}$$

and Λ is the perturbative ultraviolet cut-off (6).

Expression (A4) can be evaluated in closed form. Indeed, let us expand the exponent ${\rm e}^{-\mathcal{A}_h[\phi_{\rm inst}]}$ into a power series of βh and then integrate explicitly over ϕ_0. This yields

$$Z_{\rm inst}(h) = \sqrt{2\pi^2\alpha} \sum_{p=0}^{\infty} \frac{1}{(p!)^2} \Big(\frac{\beta h\sqrt{\alpha}}{2}\Big)^{2p} Z_p\big(\kappa {\rm e}^{-{\rm i}\theta}\big), \qquad \text{(A7)}$$

with $\kappa = \beta\,\Lambda\alpha {\rm e}^{-\alpha\pi^2}$ and

$$\begin{aligned} Z_p(\lambda) \ &= \ 1 + \sum_{w=1}^{\infty} \frac{\lambda^w}{w!} \ \prod_{m=1}^{w} \int_{|z_m|<1} \times \qquad \text{(A8)} \\ &\prod_{m=1}^{w} \frac{{\rm d}z_m \wedge {\rm d}z_m^*}{2\pi {\rm i}} \ (z_m z_m^*)^p \ \ \det \parallel G(z_i, z_j^*) \parallel \ . \end{aligned}$$

It is easy to see that $Z_p(\lambda)$ can be interpreted as a (normalized) fermionic partition function:

$$\begin{aligned} Z_p(\lambda) \ &= \ \frac{\int \mathcal{D}\bar{c}\mathcal{D}c \ {\rm e}^{-(\bar{c}\,\hat{G}^{-1}\,c) - \lambda(\bar{c},c)}}{\int \mathcal{D}\bar{c}\mathcal{D}c \ {\rm e}^{-(\bar{c}\,\hat{G}^{-1}\,c)}} = \qquad \text{(A9)} \\ &\frac{\det(\hat{G}^{-1} + \lambda)}{\det(\hat{G}^{-1})} = \det\big(1 + \lambda\,\hat{G}\big) \ , \end{aligned}$$

where the operator $\hat{G}$ acting on the Grassman fields is defined by the equation

$$\begin{aligned} &(\hat{G}c)(z, z^*) = \qquad \text{(A10)} \\ &\int_{|\zeta|<1} \frac{{\rm d}\zeta \wedge {\rm d}\zeta^*}{2\pi {\rm i}} \ (\zeta\zeta^*)^p \ G(z, \zeta)\, c(\zeta, \zeta^*) \ . \end{aligned}$$

Hence,

$$\log Z_p = {\rm Sp}\log(1 + \lambda\hat{G}) = -\sum_{s=1}^{\infty} \frac{(-1)^s}{s} \ {\rm Sp}(\hat{G}^s), \qquad \text{(A11)}$$

with

$$\begin{aligned} {\rm Sp}(\hat{G}^s) = \prod_{m=1}^{s} \Big[\int_{|z_m|<1} \frac{{\rm d}z_m \wedge {\rm d}z_m^*}{2\pi {\rm i}} \ (z_m z_m^*)^p \Big] \times \\ \big[(1 - z_1 z_2^*)(1 - z_2 z_3^*) \dots (1 - z_s z_1^*)\big]^{-1} \ . \qquad \text{(A12)} \end{aligned}$$

The small instanton problem is explicit now. Indeed, equation (A12) for $s = 1$ can be written in the form

$$\hat{\rm Sp}(\hat{G}) = \int'_{|z_1|<1} \frac{{\rm d}z_1 \wedge {\rm d}z_1^*}{2\pi {\rm i}(1 - z_1 z_1^*)} - \gamma_E - \psi(1 + p), \qquad \text{(A13)}$$

where $\psi(u) = \frac{\rm d}{{\rm d}u} \log\Gamma(u)$ and the integral diverges as $|z_1| \to 1$. This limit corresponds to small instantons – when $|z_1|$ is close to one, the solution $\phi_{\rm inst}$ (A1) with $w = 1$ is almost constant everywhere in the segment $[0, \beta]$ except for a small neighborhood of the point $\tau = \frac{\beta}{2\pi} \arg(z_1)$ where the instanton is localized. Any regularization (denoted by $\int'$ in (A13)) is essentially an instruction to suppress contributions from the small-size instantons. As a matter of fact, the Coulomb term in the action (2) provides such a suppression for any finite $\beta E_C \gg 1$. Thus the integral in (A13) should be understood as [6]:

$$\int' \dots = \int_{|z_1|<1} \frac{{\rm d}z_1 \wedge {\rm d}z_1^*}{2\pi {\rm i}} \ \frac{{\rm e}^{-\mathcal{A}_C^{(1)}}}{1 - z_1 z_1^*} \ . \qquad \text{(A14)}$$

Here

$$\mathcal{A}_C^{(1)} = \frac{\pi^2}{\beta E_C} \ \frac{1 + z_1 z_1^*}{1 - z_1 z_1^*} \qquad \text{(A15)}$$

is the value of the Coulomb term calculated on the one instanton solution ($w = 1$). Then

$$\hat{\rm Sp}(\hat{G}) = \tfrac{1}{2}\left[L + L_1\big(\tfrac{2\pi^2}{\beta E_C}\big)\right] + \log(\kappa) - \psi(1 + p), \qquad \text{(A16)}$$

where $L = 2\pi^2\alpha + O(\log\alpha)$ is some divergent temperature -independent constant. The function $L_1(x)$ is given by Eq. (32). It vanishes in the limit $\beta E_C \to \infty$.

All integrals (A12) with $s > 1$ are finite. Integrating over the phases of z_m in (A12) first, one obtains ($x_m = |z_m|^2$),

$$\begin{aligned} {\rm Sp}(\hat{G}^s) \ &= \ \Big[\prod_{m=1}^{s} \int_0^1 {\rm d}x_m \, x_m^p\Big] \ \frac{1}{1 - x_1 \cdot \ldots \cdot x_k} = \\ &\sum_{n=0}^{\infty} \Big[\int_0^1 {\rm d}x \ x^{n+p}\Big]^s = \zeta_p(s) \ , \qquad \text{(A17)} \end{aligned}$$

where $\zeta_p(s) = \sum_{n=0}^{\infty}(n+p)^{-s}$ is the generalized Riemann ζ-function. Finally, $Z_{\rm inst}(h)$ can be expressed in terms of the conventional Bessel function,

$$Z_{\rm inst}(h) = {\rm e}^{\frac{1}{2}L\lambda} \ \ \sqrt{2\pi^2\alpha} \ \Big(\frac{2\kappa}{\beta h\sqrt{\alpha}}\Big)^{\lambda} \ I_\lambda(\beta h\sqrt{\alpha}), \qquad \text{(A18)}$$

with $\lambda = \kappa e^{-i\theta}$.

Some explanations are in order at this point. First, the corrections to the saddle point formula (A4) are small in α^{-1} but they contain ultraviolet divergent integrals. Taking these divergences properly into account leads to a renormalization of the bare coupling $g_0 = (2\pi^2\alpha)^{-1}$ in Eq. (A18). The renormalization trades g_0 for the "running coupling constant" $g(\kappa)$ subject to the RG flow equation [5,14],

$$\kappa \frac{dg}{d\kappa} = 2\,g^2 + 4\,g^3 + O(g^4)\ . \qquad \text{(A19)}$$

Second, in the above derivation we took into account the instantons with positive winding numbers only. One can indeed ignore the "anti-instanton" configurations corresponding to $w < 0$ provided $\Im m(\theta) \gg 1$. Obviously, the contribution of anti-instanton fluctuations dominates when $\Im m(-\theta) \gg 1$. In this case the saddle point approximation leads to (A18) with $\lambda = \kappa e^{i\theta}$. Both limiting cases are neatly captured by the same formula if λ is understood as

$$\lambda = 2\kappa\ \cos\theta\ . \qquad \text{(A20)}$$

Equation (A20) is not easy to justify on general grounds for $\theta \sim 1$, but can be supported by means of the exact result in the case $h = 0$.

According to Ref. [22], the scaling behavior of the partition function (1) looks as follows

$$Z \to Z_{\rm scal} = e^{L\kappa\cos\theta}\ \bar{Z}(\kappa,\theta) \quad (\beta E_C,\ \alpha \to \infty), \qquad \text{(A21)}$$

where L and $\bar{Z}$ are given by Eqs. (13) and (19), respectively. We consider now the high-temperature (small-κ) expansion of (A21). Here it is useful to introduce the running coupling constant $g = g(\kappa)$ as a solution of the equation

$$\kappa = g^{-1}\ e^{-\frac{1}{2g}}\ . \qquad \text{(A22)}$$

Note that $g \ll 1$ and it solves the RG flow equation (A19) within the two-loop approximation. After a change of variables

$$y = g\,x - \log g\ , \qquad \text{(A23)}$$

the differential equation (15) can be written in the form

$$\Big[-\partial_x^2 + e^x + (g\kappa\cos\theta)^2 + \delta U(x) \Big]\ \Psi(x) = 0\,, \qquad \text{(A24)}$$

where

$$\delta U(x) = \exp\Big(\frac{e^{gx}-1}{g}\Big) - e^x - (g\kappa)^2\ . \qquad \text{(A25)}$$

For $|x| \sim 1$ the term δU is $O(g)$, so the solution Ψ_+ is approximated by the Macdonald function

$$\Psi_+(x) = 2\,g^{\frac{1}{2}}\ K_{2g\kappa\cos\theta}(2e^{\frac{x}{2}})\ \big(1 + O(g)\big)\ . \qquad \text{(A26)}$$

The normalization factor in front of K is fixed by matching (A26) to the asymptotic condition (17). As $(-x) \gg 1$, Ψ_+ takes the form

$$\Psi_+(x) \to C_+\ e^{x\kappa g\cos\theta} + C_-\ e^{-x\kappa g\cos\theta}\ . \qquad \text{(A27)}$$

The coefficient C_- is simply related to the Wronskian in Eq. (19), namely

$$W[\Psi_+,\Psi_-] = 2\kappa\cos\theta\, g^{-\kappa\cos\theta}\ C_-\ . \qquad \text{(A28)}$$

In view of (A24), one can show that the high-temperature expansion of $Z_{\rm scal}$ (A21) has the form:

$$Z_{\rm scal}\ \simeq\ e^{\kappa(L-\log g)\cos\theta}\ \ \frac{\kappa^{2\kappa\cos\theta}}{\sqrt{g}}\ \times \sum_{m=0}^{\infty} g^m\ Z_m(\kappa,\theta)\ , \qquad \text{(A29)}$$

where the coefficients $Z_m(\kappa,\theta)$ admit systematic expansions in powers of κ. In particular

$$Z_0(\kappa,\theta) = \frac{(2e^{\gamma_E})^{\kappa\cos\theta}}{\Gamma(1+2\kappa\cos\theta)}\ . \qquad \text{(A30)}$$

It is straightforward to check that the saddle point partition function $Z_{\rm inst}(0)$ is in agreement with (A30) provided λ in equation (A18) is given by (A20) and the effect of the renormalization of $g_0 = (2\pi^2\alpha)^{-1}$ is taken into account.

Let us return to Eqs. (A18), (A20) to find the magnetic susceptibility within the saddle point approximation:

$$\chi_m^{(\rm inst)}\ =\ \frac{2}{\beta^2}\ \partial_h^2 \log Z_{\rm inst}(h)\big|_{h=0} = \frac{1}{2\pi^2\alpha}\ \ \frac{1}{g(\kappa)\ (1+2\kappa\cos\theta)}\,. \qquad \text{(A31)}$$

Again the effect of renormalization has been accounted for in (A31). It is easy to see that formula (A31) is in agreement with the hypothesis that relation (22) is satisfied for any θ. Indeed, as follows from the above analysis, in the regime $\kappa \ll 1$ the potential $U(y) = \kappa^2\exp\big(e^y\big) - \kappa^2\sin^2(\theta)$ in the differential equation (15) has the effect of a rigid wall at some point $y_0 \approx -\log g$, i.e., to the left from this point, the potential is negligible, but to the right, it grows very fast, so the solution $\Psi_+(y)$ is essentially zero. More precisely, when y is below but close to y_0 the solution Ψ_+ is approximated by a linear function, $\Psi_+(y) \approx g^{-\frac{1}{2}}(y_0 - y)$. Within this "rigid wall" approximation $A_+(y_0) \approx 0$, $\partial_y A_+(y_0) \approx 0$ and $s(y_0) \gg 1$. Therefore, the RHS of Eq. (20), calculated at $y = y_0$, can be approximated by $A_-(y_0)$. In the calculation of $A_-(y)$, the solution Ψ_- needed for the integral (21) can be replaced by its asymptotics (16). This yields the relation

$$M(\kappa,\theta) \approx 2\pi^2\alpha\ \chi_m^{(\rm inst)}\ , \qquad \text{(A32)}$$

where $\chi_m^{(\rm inst)}$ is given by (A31).

[1] P. Lafarge, P. Joyez, D. Esteve, C. Urbina and M. H. Devoret, Z. Phys. B **85**, 327 (1991).
[2] G. Goeppert, H. Grabert, N.V. Prokof'ev and B.V. Svistunov, Phys. Rev. Lett. **81**, 2324 (1998).
[3] S.V. Panyukov and A. D. Zaikin, Phys. Rev. Lett. **67**, 3168 (1991).
[4] X. Wang and H. Grabert, Phys. Rev. B **53**, 12621 (1996).
[5] W. Hofstetter and W. Zwerger, Phys. Rev. Lett. **78**, 3737 (1997).
[6] I.S. Beloborodov, A.V. Andreev and A.I. Larkin, Phys. Rev. B **68**, 024204 (2003).
[7] S.L. Lukyanov and A.B. Zamolodchikov, J. Stat. Mech. **P05003** (2004).
[8] X. Wang, R. Egger and H. Grabert, Europhys. Lett. **38**, 545 (1997).
[9] J. Koenig and H. Schoeller, Phys. Rev. Lett. **81**, 3511 (1998).
[10] C. P. Herrero, G. Schon and A.D. Zaikin, Phys. Rev. B **59**, 5728 (1999).
[11] P. Werner and M. Troyer, J. Stat. Mech. **P01003** (2005).
[12] V. Ambegaokar, U. Eckern and G. Schön, Phys. Rev. Lett. **48**, 1745 (1982).
[13] G. Schoen and A. D. Zaikin, Phys. Rep. **198**, 237 (1990).
[14] J.M. Kosterlitz, Phys. Rev. Lett. **37**, 1577 (1976).
[15] G. 't Hooft, Phys. Rev. D **14**, 3432 (1976).
[16] V.A. Fateev, I.V. Frolov and A.S. Shwarz, Nucl. Phys. B **154**, 1 (1979).
[17] B.Berg and M. Lüscher, Nucl. Phys. B **190** [FS3], 412 (1981).
[18] M. Lüscher, Nucl. Phys. B **200** [FS4], 61 (1982).
[19] M. Blatter, R. Burkhalter, P. Hasenfratz and F. Niedermayer, Phys. Rev. D **53**, 923 (1996).
[20] S.E. Korshunov, Pis'ma Zh. Eksp. Theor. Phys., **45**, 342 (1987) [JETP Lett. **45**, 434 (1987)].
[21] S.L. Lukyanov, A.M. Tsvelik and A.B. Zamolodchikov, Nucl. Phys. B **719**, 103 (2005).
[22] S.L. Lukyanov, Notes on parafermionic QFT's with boundary interaction, RUNHETC-06-01, arXiv: hep-th/0606155 (2006).
[23] U. Wolff, Phys. Rev. Lett. **62**, 361 (1989).
[24] E. Luijten and H. W. K. Blöte, Int. J. Mod. Phys. C **6**, 359 (1995).
[25] A very similar phenomenon was originally observed by M. Lüscher [18] in the $O(3)$ nonlinear σ-model.
[26] M. Troyer *et al.*, Lecture Notes in Computer Science **1505**, 191 (1998); F. Alet *et al.* J. Phys. Soc. Jpn. Suppl. **74**, 30 (2005); Source codes of the libraries are available from `http://alps.comp-phys.org/` .
[27] Y.V. Nazarov, Phys. Rev. Lett. **82**, 1245 (1999).
[28] M.V. Feigelman, A. Kamenev, A.I. Larkin and M.A. Skvortsov, Phys. Rev. B **66**, 054502 (2002).